

POLYMER MATRIX COMPOSITES ON LDEF EXPERIMENTS M0003-9 and 10*

Gary L. Steckel

The Aerospace Corporation

El Segundo, CA 90245

Phone: 310/336-7116, Fax: 310/336-7055

Thomas Cookson

General Dynamics Space Systems Division

San Diego, CA 92138

Phone: 619/547-5081, Fax: 619/974-4000

Christopher Blair

Lockheed Missiles & Space Company

Sunnyvale, CA 94089-3504

Phone: 408/743-0007, Fax: 408/742-7743

ABSTRACT

Over 250 polymer matrix composites were exposed to the natural space environment on LDEF experiments M0003-9 and 10. The experiments included a wide variety of epoxy, thermoplastic, polyimide, and bismalimide matrix composites reinforced with graphite, glass or organic fibers. This paper is a review of the significant observations and test results obtained to date. Estimated recession depths from atomic oxygen exposure are reported and the resulting surface morphologies are discussed. The effects of the LDEF exposure on the flexural strength and modulus, short beam shear strength, and coefficient of thermal expansion of several classes of bare and coated composites are reviewed. Lap shear data are presented for composite-to-composite and composite-to-aluminum alloy samples that were prepared using different bonding techniques and subsequently flown on LDEF.

*Funding for the work performed by The Aerospace Corporation was processed through Air Force Space Systems Division Contract F04701-88-C-0089 under an interagency agreement with Air Force Wright Laboratory. The Lockheed Missiles & Space Company work was supported by Independent Development funds. General Dynamics Space Systems Division performed their work under an Independent Research and Development program.

INTRODUCTION

Polymer matrix composites were included in several sub-experiments of LDEF Experiment M0003, "Space Environmental Effects on Spacecraft Materials". The sub-experiments that incorporated polymer matrix composites included M0003-8, -9, -10, and -16. The polymer matrix composites (PMCs) flown on subexperiment M0003-8, a Boeing Defense and Space Group experiment, are discussed elsewhere in this conference publication (ref. 1). J. Mallon of The Aerospace Corporation is the principal investigator for M0003-16. This sub-experiment included a small number of samples relative to the other experiments and was not discussed at the workshop. However, the composites in M0003-16 had polymer matrices of polyarylacetalene and polyphenylquinoxiline that are much different from the polymer matrices included in any other LDEF experiments. Thus, the results of this experiment will undoubtedly be of great interest once they are published. The PMCs included in the remaining subexperiments, M0003-9 & 10, are discussed in this paper. M0003-9 is a Lockheed Missiles & Space Company experiment with B. Petrie serving as the principal investigator. This subexperiment included several graphite/epoxy systems. Subexperiment M0003-10, The Advanced Composites Experiment, is a joint effort between government and industry with Air Force Wright Laboratory, Flight Dynamics Laboratory, and The Aerospace Corporation, Mechanics and Materials Technology Center, serving as experimenters. General Dynamics Space Systems Division (GDSSD), Lockheed Missiles & Space Company (LMSC), Boeing Defense and Space Group, McDonnell Douglas Space Systems Company (MDSSC), and United Technologies Research Center (UTRC) also participated in this subexperiment. The experiment includes several classes of graphite fiber-reinforced polymer matrix composites. Experiment M0003-10 will be reviewed in detail, while only a brief review highlighting the experimental results will be given for the PMCs included in experiment M0003-9.

EXPERIMENT DESCRIPTION

Experiment M0003-10 consists of approximately 500 flight samples, including around 300 metal matrix composites and 200 PMCs. The metal matrix composites include graphite fiber-reinforced aluminum and magnesium and silicon carbide reinforced aluminum. The PMCs include graphite/epoxy, graphite/polysulfone, and graphite/polyimide composites. The majority of the PMCs were uncoated, but several samples were flown with various thermal control or protective coatings. The metal matrix composites were supplied by Aerospace and the organic matrix composites were supplied by GDSSD, LMSC, Boeing, and MDSSC. In addition, a

number of graphite fiber-reinforced glass matrix composites were provided by United Technologies Research Center (UTRC). Each material supplier is responsible for performing postexposure tests and analyses on their flight articles and ground control samples. Since the scope of the workshop session was limited to polymer matrix composites, no further discussion of the metal or glass matrix composites will be included in this paper. The results for these composites are discussed elsewhere (refs. 2-4).

The experiment occupied approximately one-sixth of a 6 in.-deep peripheral tray on both the leading and trailing edges of LDEF. The trays were located on LDEF Bay D, Row 4 on the trailing edge and Bay D, Row 8 on the leading edge. The samples were mounted on both sides of cassettes with one side (Deck A) exposed to the space environment and the other side (Deck B) facing inward. The environments for the samples mounted on the leading and trailing A decks were similar except those on the leading edge were also exposed to a relatively high fluence of atomic oxygen (6.6×10^{21} atoms/cm², ref. 5). Although the samples on the B decks were not exposed to the radiation environment, the experiment design was such that they experienced thermal excursions similar to those of the exposure samples. The sample cassettes were decoupled from LDEF in order to maximize the thermal excursions. For most materials, at least one sample was located on each deck and additional samples were maintained in a laboratory environment.

Although this was essentially a passive experiment, one or more samples of each class of composites was instrumented with thermistors and strain gages to monitor the thermal excursions on the leading and trailing edges and the resulting dimensional changes. The data acquisition system was set up to record temperatures and strains during the duration of an orbit once every 107 hours (approximately 78 orbits). Data were collected approximately every three minutes during the selected orbits. The data were recorded on magnetic tape until the tape was fully loaded, approximately fourteen months into the flight. No data were recorded during the unplanned final 4.5 years of the flight. The strain data are still being interpreted and will not be presented in this paper. The thermistor data indicated that the maximum and minimum temperatures for the uncoated graphite/epoxy composites were approximately +80°C and -45°C, respectively. The temperature data will be discussed in more detail below.

Most of the composite samples were 3.5 by 0.5 in. (8.9 by 1.3 cm) strips. There were also a limited number of 1 in. (2.5 cm) diameter mirror samples, a few 2.4 by 0.5 in. (6.1 by 1.3 cm) strips and several graphite/aluminum, graphite/magnesium and silicon carbide/aluminum wires. The organic matrix composites in the experiment are listed in table I. Because of the cooperative effort, a very broad test matrix of graphite/epoxy composites

having several different fiber-matrix combinations and lay ups were flown. Most of the graphite/epoxy composites were uncoated. With the exception of a T300/polyethersulfone composite, all of the graphite/thermoplastic composites had the P-1700 polysulfone matrix. Most of these composites had thermal control coatings. The remainder of the organic matrix composites had high-temperature polyimide or bismalimide matrices.

Each organization submitted a matrix of materials appropriate for studying specific phenomenon or for obtaining data on a certain composite system or set of systems. For example, the primary objective of the McDonnell Douglas experiment was to determine the effectiveness of various protective coatings for preventing property degradations in graphite/epoxy, graphite/polyimide and graphite/thermoplastic composites. Thus for each composite system, they flew uncoated control samples and those having up to three different coatings. Lockheed was interested in determining the effects of composite lay up and matrix cure temperature on the degree of thermal cycling induced microcracking. They submitted a test matrix consisting of unidirectional and cross-plyed graphite/epoxy composites having three different fiber-matrix combinations in order to achieve these objectives. Thus, the different organizations submitted separate, independent experiments, but are working together to maximize the data output of the overall experiment.

Most of the composites in the experiment were developed for space structural applications. Thus, the primary properties of interest include the flexural or tensile properties, the coefficient of thermal expansion, solar emittance and absorptance, specific heat, thermal conductivity and physical properties such as fiber volume, void content and density. Post-exposure measurements vary for the different classes of composites, but include most of the above properties as well as surface analyses, macrophotography and microstructural analyses. The remainder of the paper will include discussions of the results obtained by The Aerospace Corporation on the PMCs in M0003-10, by GDSSD on their samples in M0003-10, and by LMSC on their samples from M0003-9 & 10. The results obtained by Boeing for their samples on M0003-10 are given by P. George (ref. 1). MDSSC is very early in the evaluation of their samples so no results will be presented for their portion of M0003-10.

AEROSPACE RESULTS FOR M0003-10

The analyses performed on the PMCs at The Aerospace Corporation include preflight and post-flight photography of the cassettes and individual samples, an evaluation of the active temperature and strain data, preflight and post-flight mass measurements and scanning electron microscopy (SEM) on some of

the uncoated composites that were mounted on the leading edge.

Several observations were made from a visual inspection and by comparing preflight and post-flight photographs of the sample cassette assemblies (fig. 1). First, it was noted that all of the composites survived in excellent physical condition. Surface roughening due to atomic oxygen erosion for uncoated PMCs mounted on the exposed leading edge was the only significant visible damage. However, the erosion depth appeared to be shallow relative to the overall thickness of the affected composites. Contamination was evident on both the leading and trailing edges. For example, a large contaminated area is apparent on seven samples in the lower left corner of the leading edge cassette in the post-flight photograph of figure 1. This contamination was from another experiment or from the LDEF structure. However, there were also rainbow outgassing stains on trailing edge samples adjacent to elastomeric samples, which were from a different subexperiment of M0003 but were mounted on the Advanced Composites Experiment cassette. The most dramatic change was a yellowing or browning of many of the thermal control coatings. This was only observed for the exposed samples on the trailing edge (fig. 1). The exposed leading edge paints and those on the Deck B samples remained white. The yellowed samples were MDSSC samples having a ZnO silicone coating and the brown samples included GDSSD samples with ZnO and TiO₂ coatings and MDSSC samples with a leafing aluminum coating.

The PMC systems that were instrumented were as follows:

STRAIN GAGE ON LEADING AND TRAILING EDGES

GY70/X-30 (0/45/90/135)_{2S}
T300/934 (0)
AS/3501-6 (0)
CELION 6000/PMR-15 (0)
GR/LARC 160
T300/V378A (0/45/90/135)_{2S}
T300 FABRIC/P-1700
W-722 FABRIC/P-1700
T300/POLYSULFONE
T300/POLYETHERSULFONE

THERMISTOR ON LEADING AND TRAILING EDGES

T300/934 (0)

Plots of the maximum and minimum temperatures that were recorded on the leading and trailing edges for each of the selected orbits over the first fourteen months of the flight are shown in figure 2. The maximum and minimum temperatures on the leading edge tended to be somewhat lower than for the trailing edge. The variation in the temperature extremes as a function of orbital time was much greater, particularly for the maximum temperature,

on the leading edge. For example, the maximum temperature on the leading edge for a given orbit varied from -40°C at 65 days to 83°C at 270 days, while the lowest and highest recorded maximum temperatures on the trailing edge were -7°C and 76°C , respectively. However, the difference between the maximum and minimum temperatures for a given orbit was usually greater on the trailing edge. Thus, thermal cycling conditions were somewhat more severe on the trailing edge than on the leading edge.

The mass measurements were made after the samples had equilibrated in a constant temperature, constant humidity laboratory. Thus, moisture variations were eliminated and the only significant mass changes were those that could be attributed to atomic oxygen erosion on the exposed leading edge. The erosion depth was calculated from the known composite density and exposure area and the measured mass loss. Since the fibers and matrix have different erosion rates and densities, this technique of determining the erosion depth is an approximation. The actual erosion depths are probably somewhat higher because the samples had resin-rich surfaces and the epoxy, which has a lower density than the graphite fibers, erodes at a higher rate than the fibers. The most interesting results were for the General Dynamics composites. They flew several graphite/epoxy composites having several different fiber-matrix combinations and a wide range of fiber contents. The calculated erosion depths for these composites were inversely proportional to the fiber content (fig. 3). All of the composites provided by General Dynamics were fabricated following similar procedures. In particular, the same bleeder cloth was used so that the composites had similar surface conditions. Composites prepared by other experiment participants having significantly different surface conditions (either more matrix rich or less matrix rich) did not fall on the erosion depth versus fiber content curve established by the General Dynamics composites. Thus, it would appear that the fiber content and surface conditions are more important variables than the graphite fiber type or epoxy matrix type in determining the susceptibility of graphite/epoxy to atomic oxygen erosion. Perhaps the most important observation was that the erosion depths of the uncoated organic matrix composites were much less than for monolithic polymers. The estimated erosion depth for most of the graphite/epoxy composites was less than 0.007 cm, much less than the predicted erosion of 0.012 cm for monolithic epoxies (ref. 6) for the LDEF atomic oxygen fluence of approximately 6.6×10^{21} atoms/cm² for Row 8 (ref. 5).

The data from figure 3 are replotted in figure 4 along with the results for a graphite/polysulfone composite and for a graphite/bismalimide composite. Both of these composites were also prepared by GDSSD using the same bleeder cloth as for the graphite/epoxy composites. Note that the graphite/polysulfone

falls on the same curve as the graphite/epoxies, but the graphite/bismalimide has a much higher erosion depth for its fiber content than the other composites. In fact, the T300/V378A graphite/bismalimide composite had the highest erosion rate of all the PMCs in experiment M0003-10. This result does not necessarily indicate that bismalimide matrix composites as a class are more susceptible to atomic oxygen erosion. A graphite/bismalimide composite flown on Experiment A0175 (ref. 7) did not show excessive erosion relative to other composites included in the experiment.

Figure 5 shows SEM micrographs of the original, as fabricated surfaces of a P75S/934 graphite/epoxy composite and the T300/V378A graphite/bismalimide composite. Both composites were supplied by GDSSD and both have a 16 ply (0/45/90/135)_{2S} lay up. The woven appearance on the composites is a replication of the bleeder cloth in the resin on the composite surface. Note the bottom of the micrographs where the surface resin has chipped away revealing the outer 0° ply of graphite fibers. The 0° direction in these micrographs extends in the vertical direction. A low magnification view of the eroded leading edge samples of these composites are shown in fig. 6. The woven pattern persists on the surface even though several mils of material have been eroded away. The fact that the original surface features are maintained indicates that the erosion is uniform on a macroscopic scale. There are, however, differences in the erosion features for the two composites. Deep erosion grooves were formed on the graphite/bismalimide composite, but did not form on the graphite/epoxy composite. These grooves extend most prominently from left to right, corresponding with the direction from which the oxygen atoms approached the surface. (The velocity vector was 38° left of normal to the surfaces in the micrographs.) At a higher magnification (fig.7), major differences in the erosion features for the two composites are observed. The "Christmas tree" or cone-like erosion fragments on the graphite/epoxy sample are typical of many of the uncoated PMCs in the experiment. The rows of erosion fragments on these samples run parallel to the fiber direction with the apex of the cones or "Christmas trees" pointing in the direction of the LDEF velocity vector. The graphite/bismalimide composite formed deep erosion grooves between what appears in figure 7b to be relatively flat regions. When viewed from a different angle (fig. 8a), however, it is evident that the erosion fragments in these flat regions were finer with more of an acicular appearance and random arrangement as compared to the P75S/934 composite. The acicular erosion features, but without the deep erosion grooves, were also observed for three other composites, such as the Celion 6000/PMR-15 graphite/polyimide composite shown in figure 8b. This composite also has a "spider web" or "hair net" ash-like material on the surface. All of the uncoated PMCs in Experiment M0003-10 had erosion features showing the coarse, "Christmas tree"

structure or the fine, needle structure as indicated in table II. An attempt was made to correlate the type of erosion features with the graphite fiber type, matrix type, or lay up. The only correlation that could be made was that all of the composites that had the coarse "Christmas tree" features had high-modulus GY70 (70×10^6 psi modulus) or P75S (75×10^6 psi modulus) fibers while the composites with the fine, needle structure had low-modulus T300 or Celion 6000 fibers (both having a $30-35 \times 10^6$ psi modulus). This correlation is not presented as proof that the fiber type controls the appearance of the atomic oxygen erosion features. In fact, the correlation is somewhat surprising since the GY70 fiber, which is processed from a polyacrylonitrile precursor, and the P75S fiber, which is processed from a mesophase pitch precursor, have much different structures. It is hoped that these observations will encourage further investigations into the origins of the different types of atomic oxygen erosion features found on the LDEF PMCs.

GDSSD RESULTS FOR M0003-10

As indicated in table I, GDSSD provided GY70/X-30, GY70/CE-339, P75S/CE-339, P75S/934 and GY70/934 graphite/epoxy, W-722/P-1700 graphite/glass/polyethersulfone and T300/V378A graphite/bismalimide composites. The GY70/X-30 was flown bare and with a Sn-In eutectic alloy moisture barrier coating and the W-722/P-1700 was flown bare and with thermal control coatings. All of the other composites were flown with no coating. All of the GDSSD composites had a (0/45/90/135)_{2S} lay up except for those having the W-722 woven graphite/glass fabric as a reinforcement. The coated W-722/P-1700 composites included lap shear samples that had been spot welded together. All of the other GDSSD composites were 3.5 in. by 0.5 in. strips.

GDSSD performed flexural tests to determine the flexural strength and modulus and short beam shear tests for the strip samples and lap shear strength measurements for the spot welded samples. A bar graph showing the ultimate flexural strength results for each sample for the P75S/934 composite is shown in figure 9. All of the samples had similar strength values except for those that were subjected to atomic oxygen erosion on the leading edge. In order to show the true loss in load carrying ability, the strength and modulus calculations for the leading edge samples were based upon the original area of the samples. There was no apparent loss in strength relative to the laboratory controls for the samples mounted on the interior of the cassettes or those mounted on the outer trailing edge. There was also no loss in strength relative to the average preflight value, indicated by the INITIAL value marked on the ordinate. The results for this composite are typical of the flexural strength,

flexural modulus, and short beam shear strength data for all of the uncoated GDSSD composites. That is, there was no reduction in mechanical properties except that due to atomic oxygen erosion on the leading edge. In order to quantify the property loss on the leading edge, the average property value for the leading edge samples was divided by the average value for all of the remaining samples (laboratory controls, all deck B samples, and trailing edge deck A samples). This gave a normalized strength for the leading edge for all of the GDSSD uncoated composites as presented in figure 10. The five graphite/epoxy composites all had normalized leading edge strength values that were at least 70% of the original value, about as expected considering that the outer 0° ply was mostly or completely eroded away. The T300/V378A graphite/bismalimide composite strength on the leading edge was only 40% of the original strength. The mass loss for this material was somewhat greater than for the other composites, but not to the extent that one would expect such a large loss of strength.

The flexural modulus results for the leading edge are shown in figure 11. The T300/V378A composite also showed the largest modulus reduction, along with the P75S/934 composite at approximately 65% of the original modulus. But the reduction in the modulus was not nearly as great as for the strength. All of the composites showed only a 10% reduction in the short beam shear strength as indicated in figure 12. This is not surprising since short beam shear strength is not as sensitive to surface degradation as are flexural properties.

The lap shear strength results for the spot welded W-722/P-1700 composites with the ZnO coating are shown in figure 13. There was an insufficient number of samples to allow any comparisons between the different exposure conditions. However, it is apparent that there was no reduction in strength as all but one sample had a higher strength than the average value measured prior to the flight. Similar results were obtained for W-722/P-1700 composites with the TiO₂ coating.

LMSC RESULTS FOR M0003-9 AND 10

All of the composites flown by LMSC had epoxy matrices. Most of the LMSC composites were reinforced with graphite fibers, but one set of samples was reinforced with DuPont's Kevlar 49 aramid fibers and two sets of composites were reinforced with E-Glass fibers. A listing of the LMSC composites is given in table III and includes the prepreg supplier for each system. The Lockheed experiment included a wide variety of epoxy matrix composites. The epoxy matrices had a wide range of cure temperatures and glass transition temperatures and the fibers ranged from the

relatively low-modulus E-Glass to the high-modulus P75 and GY70 graphite fibers. The HMS/3501, GY70/X904B, and E-Glass/X904B composites were flown on subexperiment 10 and all the rest of the LMSC composites were on subexperiment 9. The subexperiment 9 composite strips were 3.5 in. long by 0.75 in. wide, which is the same length but 0.25 in. wider than the subexperiment 10 strips. In addition to strips, the LMSC experiment also included double lap shear samples of HMF 330/934 graphite fabric reinforced epoxy bonded to 2024 aluminum with Hysol 9628 epoxy film adhesive.

Subexperiment 9 was located on Bay D, Row 3 on the trailing edge of LDEF and Bay D, Row 9 on the leading edge. Most of the samples were mounted facing outward so that they were exposed to the full space environment, but a few of the samples were covered so that they were protected from radiation and atomic oxygen.

The LMSC analyses and property measurements include macrophotography, mass loss measurements, SEM surface morphology of eroded surfaces and impact damage, microphotography of microcrack formation, ESCA contamination analysis, short beam shear strength, flexural strength and modulus, double lap shear strength, and coefficient of thermal expansion (CTE) measurements. This paper includes the mechanical property and CTE results.

The results of the flexural testing are given in table IV. None of the composites show any clear variation in strength or modulus between the exposure samples and the laboratory controls. For the leading edge samples which experienced a loss of material from atomic oxygen, LMSC based their strength and modulus calculations on the final thickness of the composites. Thus, their results show that the strength and modulus of the composites were unaffected by the mass loss. However, for a real structure, one would need to determine the effect of the mass loss on the load carrying capability and stiffness. GDSSD based their calculations on the initial thickness, which partially accounts for the fact that they measured a reduction in strength and modulus while LMSC did not. In addition to the different approaches in defining the sample thickness, the composite lay ups were also significantly different between the GDSSD and LMSC samples. All of the GDSSD composites had a 0° ply at the surface, whereas all of the LMSC samples had a 45° ply at the outer surface. In a flexural test, the loss of a 0° ply from the surface will have a much more pronounced effect on the strength than the loss of a 45° ply. Thus, mass losses from atomic oxygen would be expected to affect the flexural properties of the GDSSD composites to a greater extent than for the LMSC composites. In assessing the effect of atomic oxygen erosion on the strength and modulus of composites, the composite lay up is an important consideration.

Short beam shear strength measurements were made on ten different unidirectional composites as shown in table V. The short beam shear strength ranged from a low value of less than 4 Ksi for a Kevlar 49/X904B composite to a high of nearly 13 Ksi for T50/F263 composites. The LDEF exposure had no apparent effect on the short beam shear strength for any of the epoxy matrix composites. Here again, the LMSC strength calculations were based upon the final area which accounts for the fact that they did not report a strength reduction for the leading edge, whereas GDSSD reported a small strength reduction based upon the initial area.

Table VI shows the shear strength results for the HMF 330/934//Hysol 9628 Adhesive//2024 Aluminum double lap shear samples. Four samples were tested for each flight condition along with eight control samples. There was no apparent reduction in shear strength for the leading edge exposure or for the flight controls as compared to the laboratory control samples. The trailing edge exposure resulted in approximately a 25% reduction in lap shear strength.

CTE measurements were made using a quartz dilatometer on four unidirectional graphite/epoxy composites as indicated in table VII. Within the accuracy of the technique, there were no significant changes in the CTE for any of the composites.

SUMMARY

The findings to date for LDEF Experiments M0003-9 and 10 on polymer matrix composites may be summarized as follows.

The Aerospace Corporation Results

1. Atomic oxygen erosion depths are in the range from 0.0015 to 0.0035 in. (0.0038 to 0.0089 cm) based upon mass loss measurements.
2. Atomic oxygen erosion depth is an inverse function of fiber content for graphite/polymer composites.
3. Two types of atomic oxygen erosion morphologies were observed for graphite/polymer composites. Preliminary observations suggest that the erosion features may be a function of the fiber modulus or structure.

General Dynamics Space Systems Division Results

1. Atomic oxygen erosion on the leading edge of LDEF resulted in a 20-30% reduction in the strength and modulus for uncoated graphite/epoxy composites. An uncoated graphite/bismalimide

composite, T300/V378A had a 60% reduction in strength.

2. Atomic oxygen erosion on the leading edge resulted in a 10% reduction in short beam shear strength for uncoated graphite/epoxy and T300/V378A composites.
3. There were no significant changes in the flexural strength or modulus or short beam shear strength for any uncoated composites on the trailing edge of LDEF or for flight control samples.
4. There were no significant changes in the flexural strength or modulus or short beam shear strength for any composites having thermal control or Sn-In coatings. These coatings, provided protection from atomic oxygen.
5. The lap shear strength of spot welded W-722/P-1700 composites having ZnO or TiO₂ coatings was unaffected by exposure on the leading or trailing edges of LDEF.

Lockheed Missiles And Space Company Results

1. The extended LDEF exposure had no effect on the flexural strength or modulus or the short beam shear strength of any of the LMSC epoxy matrix composites.
2. The lap shear strength for an HMF330/934 composite bonded to 2024 aluminum with Hysol 9628 epoxy film adhesive was reduced by approximately 25% by exposure on the trailing edge of LDEF as compared to laboratory control samples. There was no effect on the shear strength for samples exposed on the leading edge or for flight control samples.
3. The LDEF exposure did not have a significant effect on the coefficient of thermal expansion of unidirectional GY70/CE-339, T50/F263, T50/934, or T50/X904B graphite/epoxy composites.

REFERENCES

1. George, P.: Space Environmental Effects on LDEF Low-Earth Exposed Graphite-Reinforced Polymer-Matrix Composites. LDEF Materials Workshop '91, NASA CP-3162, 1992.
2. Steckel, G. L. and Le, T. D.: M0003-10: LDEF Advanced Composites Experiment. First LDEF Post-Retrieval Symposium, NASA CP-3134, 1992, pp. 1041-1053.
3. Tredway, W. K. and Prewo, K. M.: Analysis of the Effect of Space Environmental Exposure on Carbon Fiber Reinforced Glass. United Technologies Research Center Report R91-112542-4, May, 1991.
4. Steckel, G. L. and Le, T. D.: Composites Survive Space Exposure. Advanced Materials and Processes, vol. 139, no.8, August, 1991. pp. 35-38.
5. Bourassa, R. J.; Gillis, J. R.; and Rousslang, K. W.: Atomic Oxygen and Ultraviolet Radiation Mission Total Exposures For LDEF Experiments. First LDEF Post-Retrieval Symposium, NASA CP-3134, 1992, pp. 643-661.
6. Banks, B. A.: Atomic Oxygen Interaction with Materials on LDEF. LDEF Materials Data Analysis Workshop, NASA CP 10046, July 1990, pp. 191-216.
7. Vyhnal, R.: Evaluation of Long-Duration-Exposure to the Natural Space Environment on Graphite-Polyimide and Graphite-Epoxy Mechanical Properties. LDEF Materials Workshop '91, NASA CP-3162, 1992.

TABLE I.- LIST OF ORGANIC MATRIX COMPOSITES

MATERIAL DESCRIPTION FIBER/MATRIX/COATING	LAY UP	SUPPLIER	NUMBER OF SAMPLES					
			LEADING		TRAILING		CONTROL	
			A	B	A	B	A	B
<u>GRAPHITE/EPOXY STRIPS</u>								
GY70/X-30/NONE, Sn-In	(0/45/90/135) ^{2S}	GDSSD	4	4	3	3	5	
GY70/X904B	(0) ¹⁶ , (0/90 ₂ /0) ^{2S}	LMSC	3	3	3	3	0	
GY70/934	(0/45/90/135) ^{2S}	GDSSD	2	3	2	2	7	
GY70/CE-339	(0/45/90/135) ^{2S}	GDSSD	2	3	3	3	6	
P75S/CE-339	(0/45/90/135) ^{2S}	GDSSD	2	3	2	2	8	
P75S/934	(0/45/90/135) ^{2S}	GDSSD	2	2	2	2	8	
T300/5208/NONE, ZnO, Al FLAKE	(0) ¹⁶	MDSSC	1	2	2	3	0	
T300 TAPE/934	(0) ¹⁶	BOEING	3	3	3	3	4	
AS/3501-6	(0) ¹⁶	BOEING	3	3	3	3	3	
HMS/3501-5A	(0) ¹⁶ , (0/90 ₂ /0) ^{2S}	LMSC	2	2	0	0	0	
E-GLASS FABRIC/X904B	(0) ¹⁶	LMSC	1	1	1	1	0	
<u>GRAPHITE/THERMOPLASTIC STRIPS</u>								
T300 FABRIC/P-1700 PS	(0/90) ⁸	BOEING	3	3	3	3	4	
T300/P-1700 PS/NONE, TiO ₂ , ZnO, LEAFING Al		MDSSC	4	0	0	0	0	
T300/PES/NONE, TiO ₂ , ZnO, LEAFING Al		MDSSC	1	0	5	2	0	
W-722 FABRIC/P-1700 PS/NONE, TiO ₂ , ZnO	(0/90) ⁸	GDSSD	15	11	15	11	12	
<u>GRAPHITE/POLYIMIDE STRIPS</u>								
GRAPHITE/LARC 160	(0) ¹⁶	BOEING	2	3	2	3	5	
CELION 6000/PMR-15	(0) ¹⁶	BOEING	3	1	2	3	4	
CELION 6000/PI/NONE, ZnO		MDSSC	1	0	1	0	0	
T300/V378A (BISMALIMIDE)	(0/45/90/135) ^{2S}	GDSSD	3	3	3	3	4	

W-722 is a graphite/glass fabric.

The control samples listed were stored at The Aerospace Corporation. For those composites for which no control samples are listed, the controls were stored at the supplier's facility and were not included in The Aerospace Corporation records.

TABLE II.-ATOMIC OXYGEN EROSION FEATURES FOR POLYMER MATRIX COMPOSITE

<u>OBSERVED EROSION FEATURES</u> COMPOSITE SYSTEM	COMPOSITE SUPPLIER
<u>COARSE, CHRISTMAS TREE STRUCTURE</u>	
GY70/X904B	LMSC
GY70/X-30	GDSSD
GY70/CE-339	GDSSD
GY70/934	GDSSD
P75S/934	GDSSD
P75S/CE-339	GDSSD
<u>FINE, NEEDLE STRUCTURE</u>	
T300/934	BOEING
T300/V378A*	GDSSD
T300 FABRIC/P-1700	BOEING
CELION 6000/PMR-15**	BOEING
GR/LARC 160**	BOEING
T300/POLYSULFONE**	MDSSC
<u>TRANSITIONAL STRUCTURE</u>	
T300/POLYETHERSULFONE	MDSSC

- * Deep Erosion Grooves
- ** Spider Web Pattern On Surface

TABLE III.- LIST OF LMSC COMPOSITES IN EXPERIMENTS M0003-9 & 10

<u>MATERIAL DESCRIPTION</u> FIBER/MATRIX	LAY UP ORIENTATION	PREPREG SUPPLIER
GY70/CE-339	(0) ₁₆ & (45/-45 ₂ /45) _{4T}	FERRO
T50/F263	(0) ₁₆ & (45/-45 ₂ /45) _{4T}	HEXCELL
T50/934	(0) ₁₆ & (45/-45 ₂ /45) _{4T}	FIBERITE
T50/X904B	(0) ₁₆ & (45/-45 ₂ /45) _{4T}	FIBERITE
T50/E788	(0) ₁₆ & (45/-45 ₂ /45) _{4T}	HEXCELL
P75/934		FIBERITE
P75/F593		HEXCELL
HMS/3501	(0) ₁₆ & (45/-45 ₂ /45) _{4T}	NARMCO
CELION 6000/E788	(0) ₁₆ & (45/-45 ₂ /45) _{4T}	HEXCELL
HMF 176/934 FABRIC	(0) ₁₆ & (+45) _{4S}	FIBERITE
GY70/X904B	(0) ₁₆ & (45/-45 ₂ /45) _{4T}	FERRO
KEVLAR 49/X904B FABRIC	(0) ₁₆ & (+45) _{4S}	FIBERITE
E-GLASS/CE-339	(0) ₁₆	FERRO
E-GLASS/X904B	(0) ₁₆	FERRO

TABLE IV.-FLEXURAL TEST DATA FOR LMSC COMPOSITES

<u>MATERIAL DESCRIPTION</u> SAMPLE LOCATION	FLEXURAL STRENGTH (KSI)	FLEXURAL MODULUS (MSI)
<u>GY70/CE-339 (45/-45₂/45)_{4T}</u>		
LEADING EDGE	35.2	2.14
TRAILING EDGE	37.9	2.55
LAB CONTROL	38.2	2.48
<u>GY70/X904B (45/-45₂/45)_{4T}</u>		
LEADING EDGE	-----DAMAGED SAMPLE-----	
TRAILING EDGE	21.1	1.50
FLIGHT CONTROL (LEADING)	22.1	1.80
FLIGHT CONTROL (TRAILING)	22.4	1.60
LAB CONTROL	23.6	2.00
<u>T50/F263 (350^{OF} CURE) (45/-45₂/45)_{4T}</u>		
LEADING EDGE	49.4	3.49
TRAILING EDGE	47.0	3.14
LAB CONTROL	47.7	3.26
<u>T50/F263 (300^{OF} CURE) (45/-45₂/45)_{4T}</u>		
LEADING EDGE	55.9	3.61
TRAILING EDGE	51.4	3.39
LAB CONTROL	54.4	3.56
<u>T50/934 (45/-45₂/45)_{4T}</u>		
LEADING EDGE	48.7	2.71
TRAILING EDGE	52.1	3.01
LAB CONTROL	48.3	2.90
<u>T50/X904B (45/-45₂/45)_{4T}</u>		
LEADING EDGE	46.3	2.29
TRAILING EDGE	40.0	1.97
LAB CONTROL	47.1	2.31
<u>HMF 176/934 FABRIC (+/-45)_{4S}</u>		
LEADING EDGE	66.8	3.16
TRAILING EDGE	67.6	3.14
LAB CONTROL	67.0	3.23
<u>KEVLAR 49/X904B FABRIC (+/-45)_{4S}</u>		
LEADING EDGE	28.4	1.10
TRAILING EDGE	24.4	0.93
LAB CONTROL	26.9	1.16

TABLE V.-SHORT BEAM SHEAR DATA FOR LMSC COMPOSITES

<u>MATERIAL DESCRIPTION</u> SAMPLE LOCATION	SHORT BEAMS SHEAR STRENGTH (KSI)
<u>GY70/CE-339 (0)₁₆</u>	
LEADING EDGE	8.6
TRAILING EDGE	8.1
LAB CONTROL	7.6
<u>GY70/X904B (0)₁₆</u>	
LEADING EDGE	8.2
TRAILING EDGE	8.5
FLIGHT CONTROL (LEADING)	8.6
FLIGHT CONTROL (TRAILING)	8.5
LAB CONTROL	8.4
<u>T50/F263 (0)₁₆</u>	
LEADING EDGE	12.7
TRAILING EDGE	12.6
LAB CONTROL	12.6
<u>T50/934 (0)₁₆</u>	
LEADING EDGE	11.8
TRAILING EDGE	12.1
LAB CONTROL	10.0
<u>T50/X904B (0)₁₆</u>	
LEADING EDGE	10.6
TRAILING EDGE	10.8
LAB CONTROL	7.7
<u>HMF 176/934 FABRIC (0)₁₆</u>	
LEADING EDGE	10.9
TRAILING EDGE	12.1
LAB CONTROL	10.7
<u>KEVLAR 49/X904B FABRIC (0)₁₆</u>	
LEADING EDGE	3.6
TRAILING EDGE	3.8
LAB CONTROL	3.7
<u>HMS/3501 (0)₁₆</u>	
LEADING EDGE	7.1
FLIGHT CONTROL (LEADING)	7.6
CONTROL	6.7
<u>E-GLASS/CE-339 (0)₁₆</u>	
LEADING EDGE	7.4
TRAILING EDGE	7.4
CONTROL	7.1
<u>E-GLASS/X904-B (0)₁₆</u>	
LEADING EDGE	8.7
TRAILING EDGE	9.0
FLIGHT CONTROL (LEADING)	8.9
FLIGHT CONTROL (TRAILING)	9.0
CONTROL	8.3

TABLE VI.-LMSC DOUBLE LAP SHEAR STRENGTH DATA

HMF 330/934 BONDED TO 2024 ALUMINUM WITH HYSOL 9628 EPOXY FILM ADHESIVE

SAMPLE LOCATION	DOUBLE LAP SHEAR STRENGTH (PSI) SAMPLE	AVERAGE
CONTROL	4020	
CONTROL	3910	
CONTROL	4210	
CONTROL	4260	
CONTROL	4060	4080±110
CONTROL	4090	
CONTROL	4040	
CONTROL	4040	
LEADING EDGE	4290	
LEADING EDGE	3780	
LEADING EDGE	3270	3850±440
LEADING EDGE	4040	
FLIGHT CONTROL (LEADING)	3960	
FLIGHT CONTROL (LEADING)	4250	
FLIGHT CONTROL (LEADING)	4190	4110±140
FLIGHT CONTROL (LEADING)	4020	
TRAILING EDGE	3240	
TRAILING EDGE	2910	
TRAILING EDGE	3280	2910±500
TRAILING EDGE	2190	
FLIGHT CONTROL (TRAILING)	4130	
FLIGHT CONTROL (TRAILING)	4230	
FLIGHT CONTROL (TRAILING)	4170	4160±60
FLIGHT CONTROL (TRAILING)	4100	

TABLE VII.-COEFFICIENT OF THERMAL EXPANSION DATA FOR LMSC COMPOSITE

<u>MATERIAL DESCRIPTION</u> <u>SAMPLE LOCATION</u>	THERMAL EXPANSION (PPM/°C)
<u>GY70/CE-339 (0)₁₆</u>	
LEADING EDGE	-0.93
TRAILING EDGE	-0.98
CONTROL	-0.93
<u>T50/F263 (0)₁₆</u>	
LEADING EDGE	-0.30
TRAILING EDGE	-0.51
CONTROL	-0.50
<u>T50/934 (0)₁₆</u>	
LEADING EDGE	-0.59
TRAILING EDGE	-0.63
CONTROL	-0.23
<u>T50/X904B (0)₁₆</u>	
LEADING EDGE	-0.47
TRAILING EDGE	0.10
CONTROL	-0.27

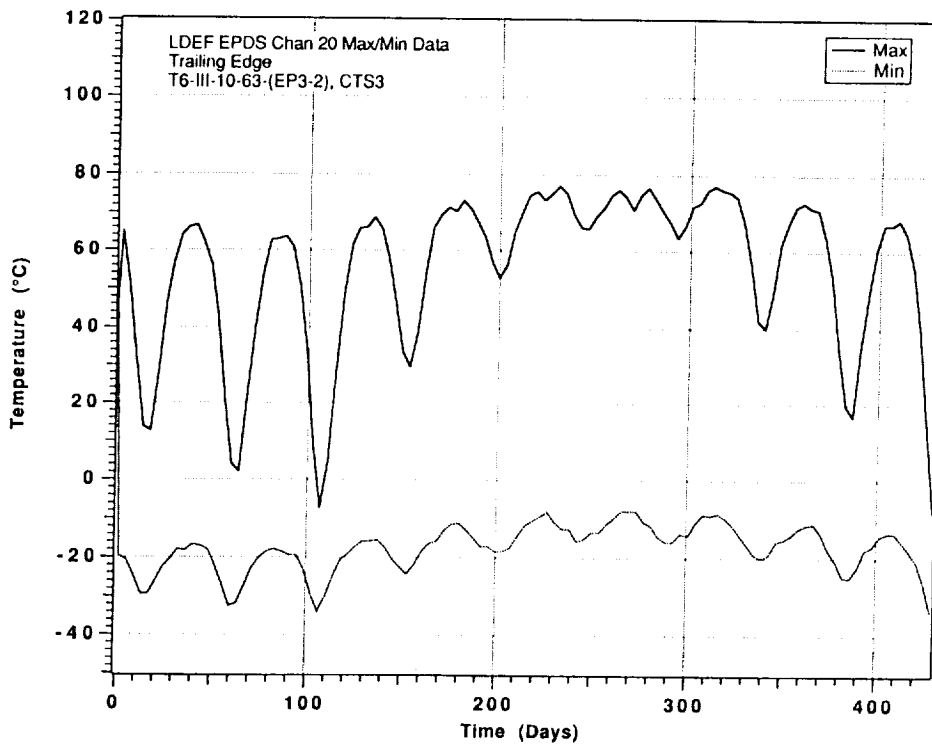
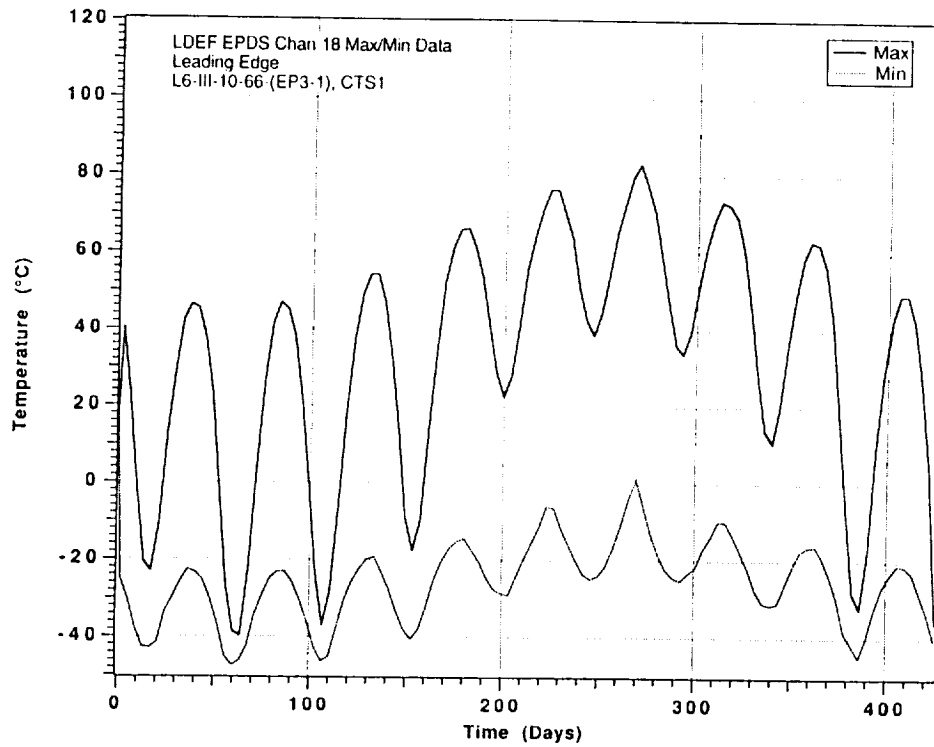
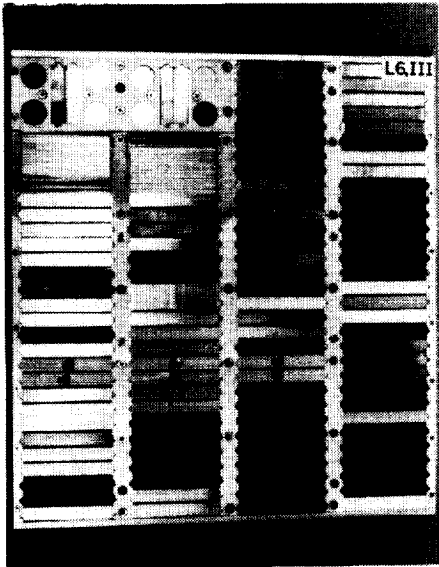


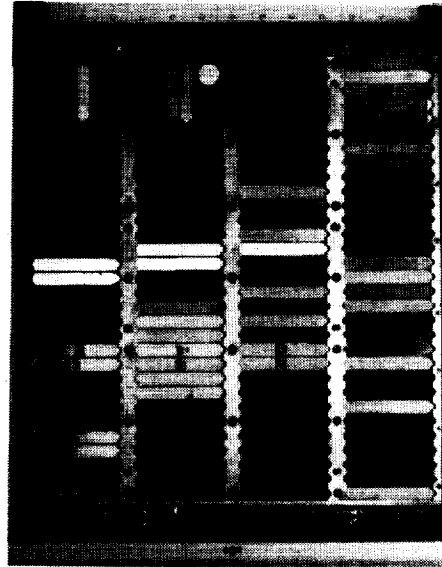
Figure 1. Maximum and Minimum Temperature Recorded for Each Orbit for T300/934 Graphite/Epoxy Samples Mounted on the Leading and Trailing Edges of LDEF.

LEADING EDGE EXPOSED

PREFLIGHT

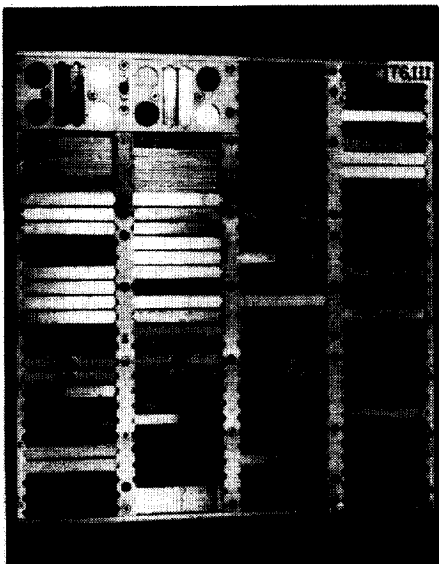


POSTFLIGHT



TRAILING EDGE EXPOSED

PREFLIGHT



POSTFLIGHT

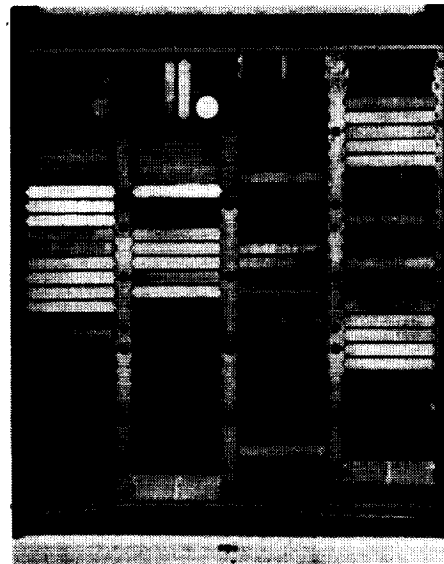


Figure 2. Preflight and Post-Flight Photographs of Exposed Side of Leading Edge and Trailing Edge Sample Cassettes.

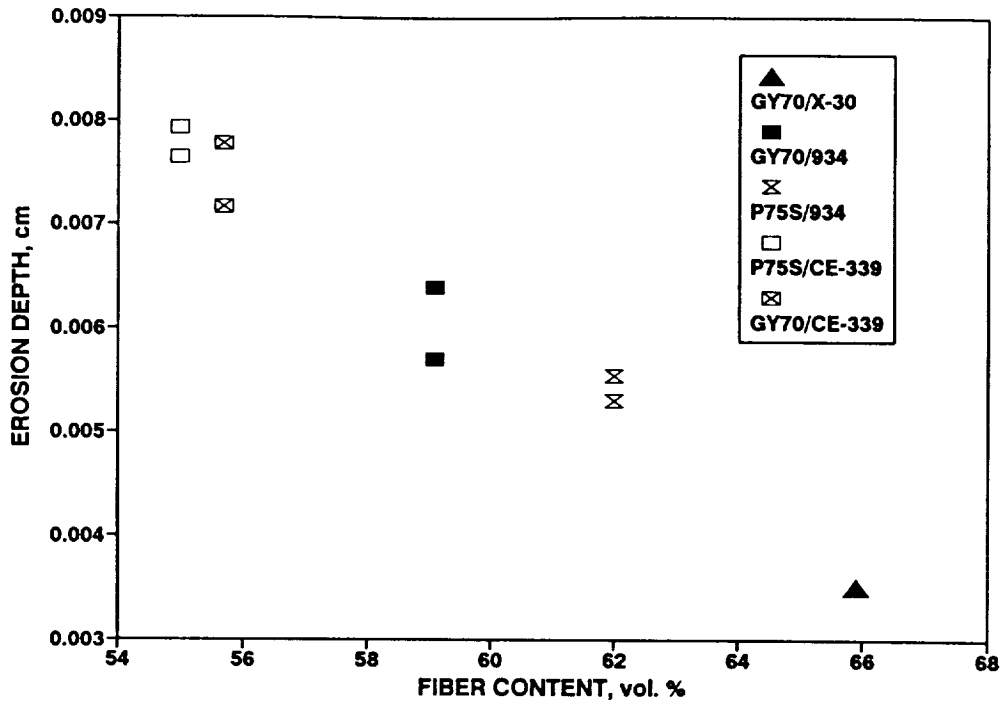


Figure 3. Estimated Atomic Oxygen Erosion Depth Versus Fiber Content for Several GDSSD Graphite/Epoxy Composite Systems.

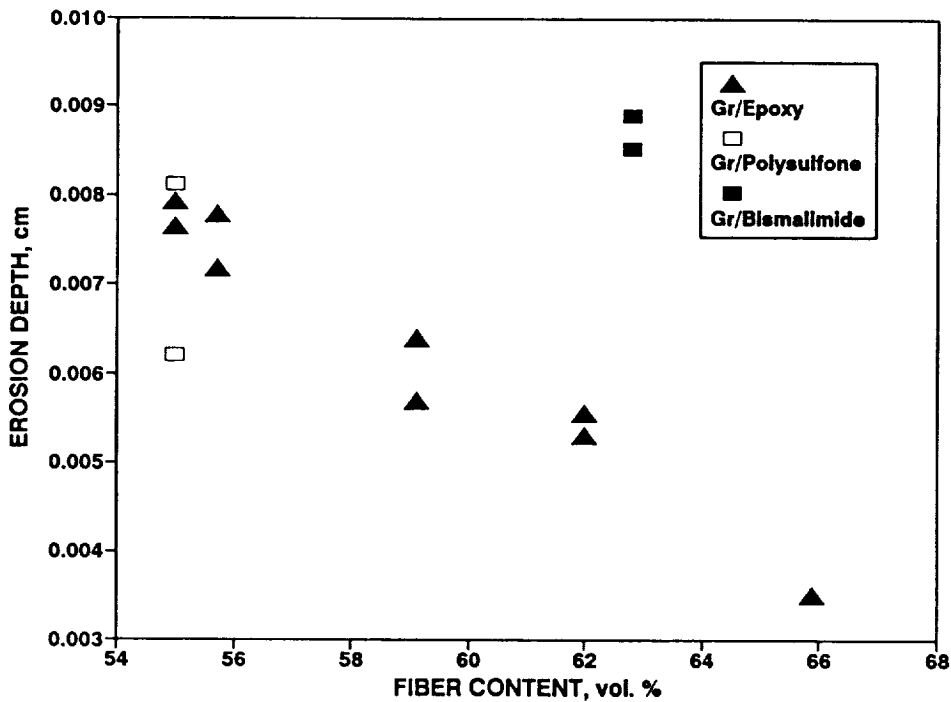
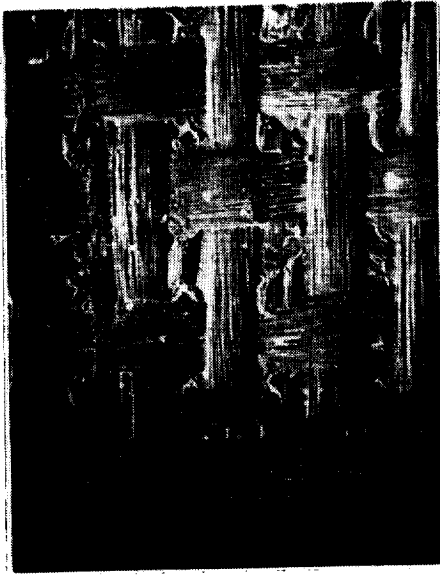
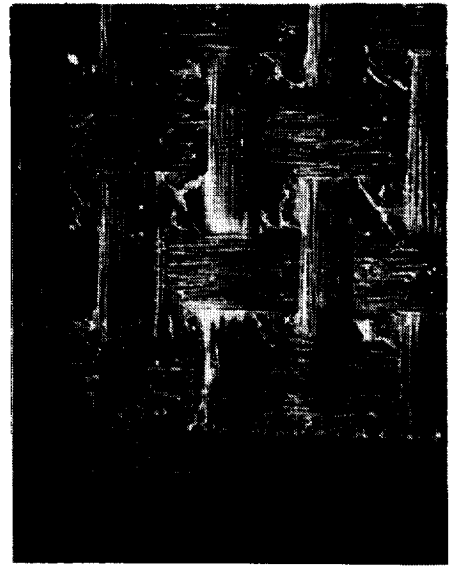


Figure 4. Estimated Atomic Oxygen Erosion Depth Versus Fiber Content for Several GDSSD Graphite/Epoxy, Graphite/Polysulfone, and Graphite/Bismalimide Composite Systems.

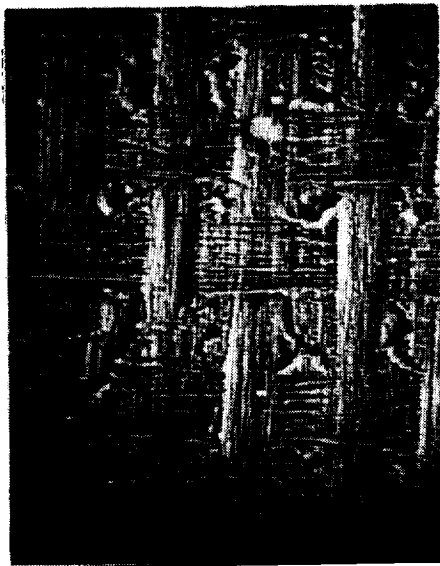


(a)

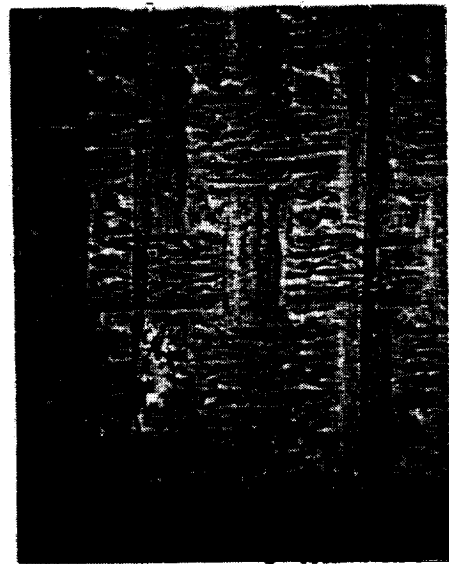


(b)

Figure 5. Scanning Electron Micrographs of Initial Surfaces of (a) P75S/934 Graphite/Epoxy Composite and (b) T300/V378A Graphite/Bismalimide Composite.

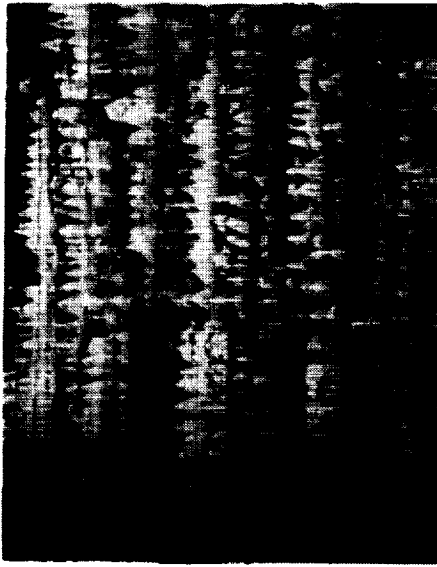


(a)

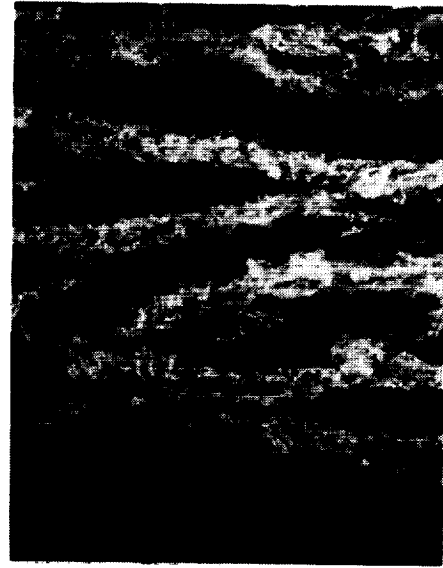


(b)

Figure 6. Low-Magnification Scanning Electron Micrographs of Eroded Surfaces of (a) P75S/934 Graphite/Epoxy Composite and (b) T300/V378A Graphite/Bismalimide Composite.



(a)

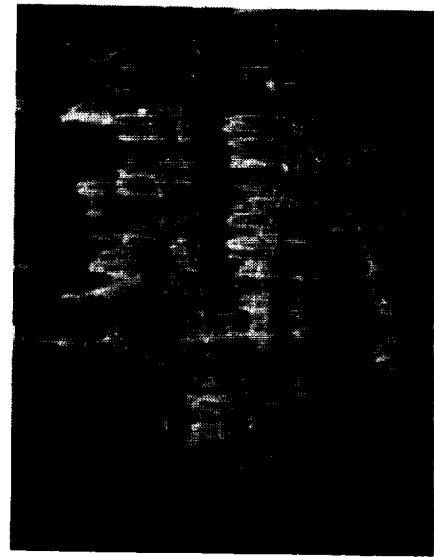


(b)

Figure 7. High-Magnification Scanning Electron Micrographs of Eroded Surfaces of (a) P75S/934 Graphite/Epoxy Composite and (b) T300/V378A Graphite/Bismalimide Composite.



(a)



(b)

Figure 8. High-Magnification Scanning Electron Micrographs of Eroded Surfaces of (a) T300/V378A Graphite/Bismalimide Composite at a Different Angle From Figure 7a and (b) Celion 6000/PMR-15 Graphite/Polyimide Composite.

ULTIMATE STRENGTH(KSI)

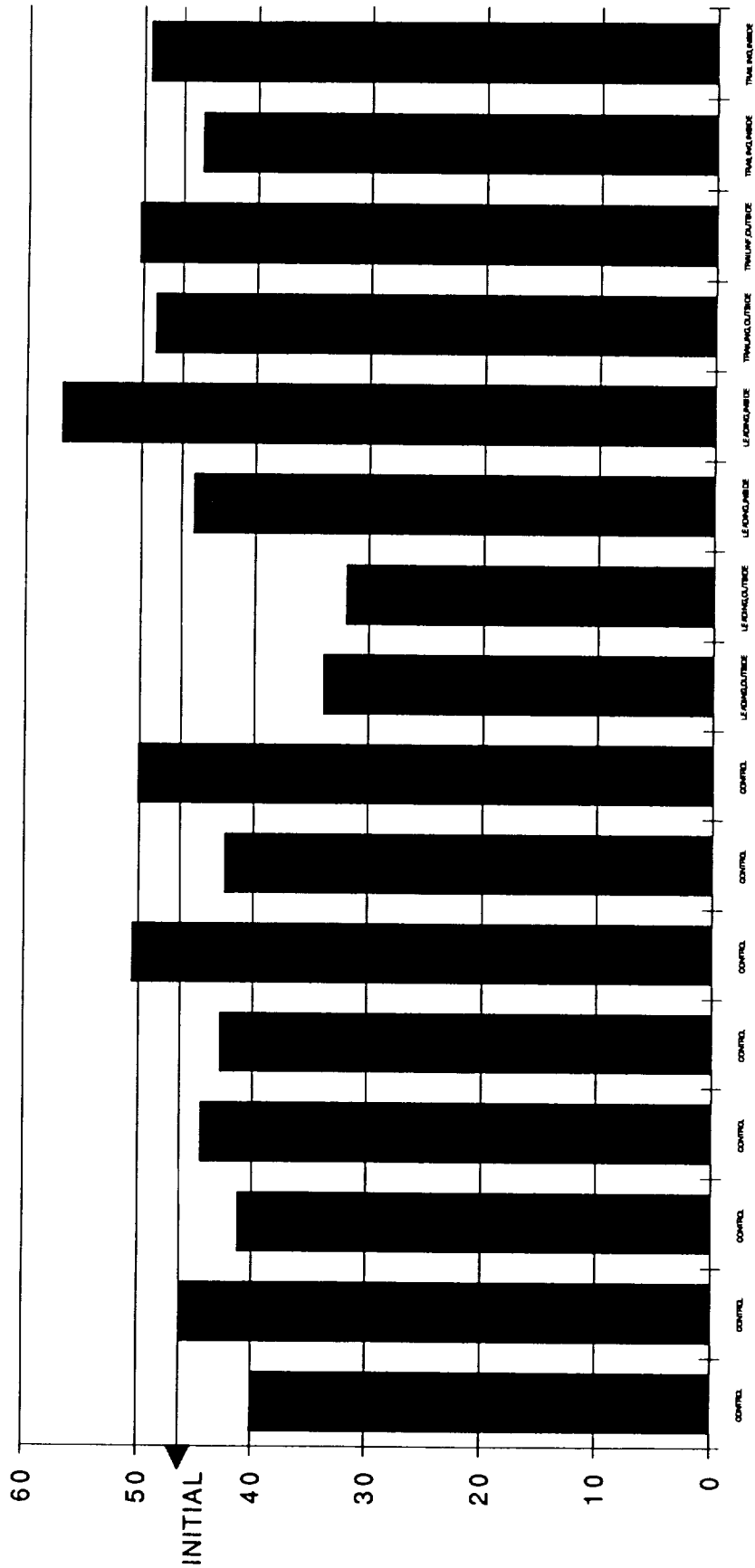


Figure 9. Bar Graph Showing Flexural Strength Data For All Samples for GDSSD P75S/934 Graphite/Epoxy Composite.

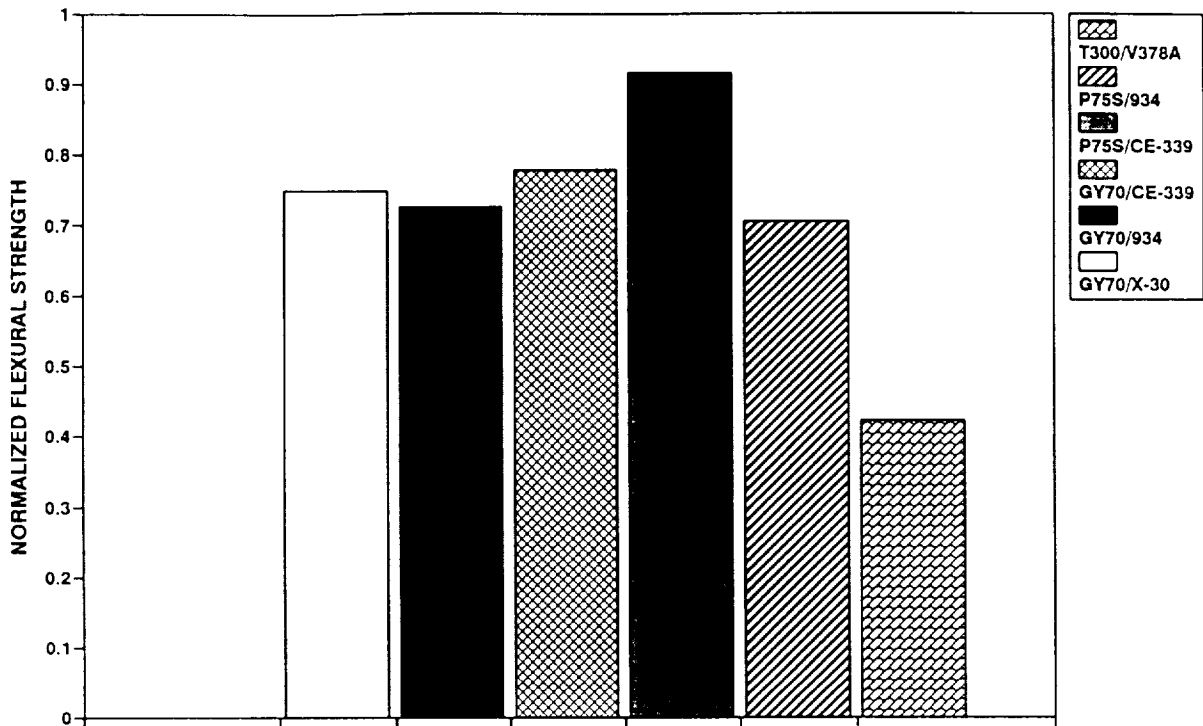


Figure 10. Bar Graph Showing Reduction in Flexural Strength for Uncoated GDSSD Composites on the Leading Edge of LDEF.

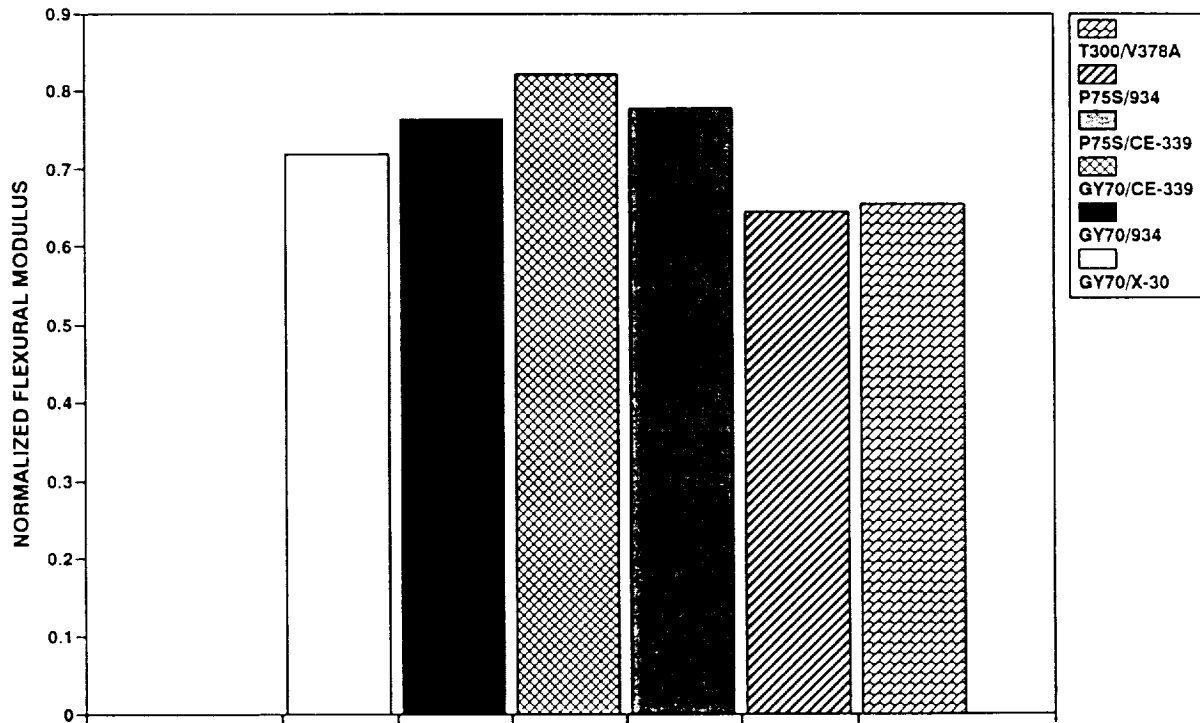


Figure 11. Bar Graph Showing Reduction in Flexural Modulus for Uncoated GDSSD Composites on the Leading Edge of LDEF.

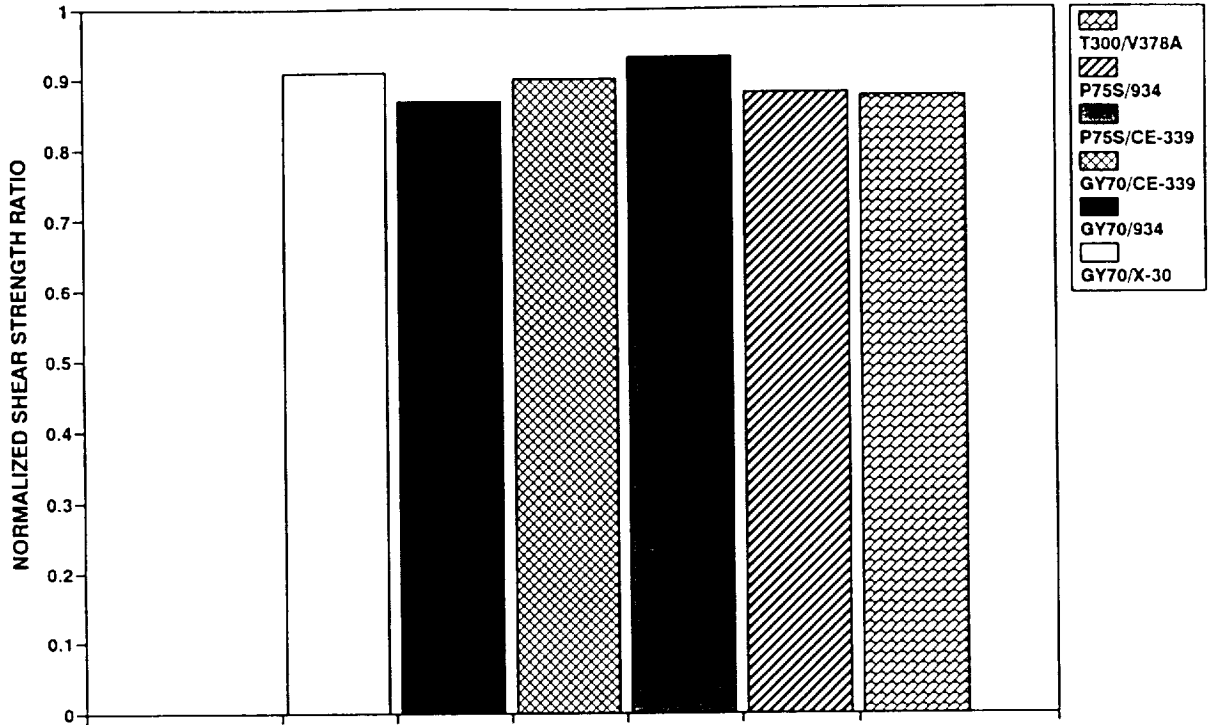


Figure 12. Bar Graph Showing Reduction in Short Beam Shear Strength for Uncoated GDSSD Composites on the Leading Edge of LDEF.

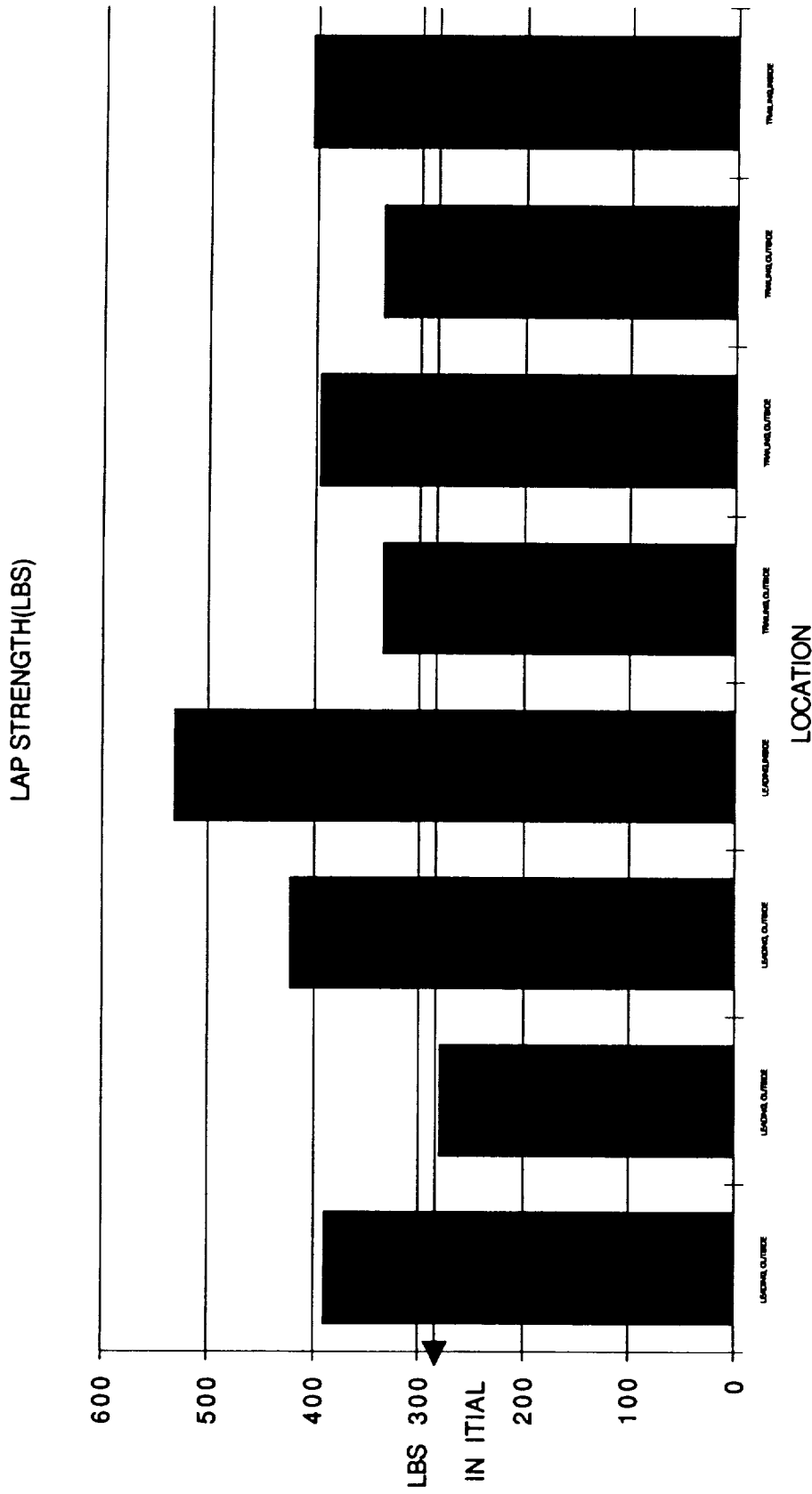


Figure 13. Bar Graph Showing Lap Shear Strength Data For All Samples for GDSSD Spot Welded W722/P-1700 Composites with a ZnO Coating.